

High-energy collisions inside black holes and their counterpart in flat space-time

O. B. Zaslavskii

*Department of Physics and Technology,
Kharkov V.N. Karazin National University,
4 Svoboda Square, Kharkov 61022, Ukraine**

Two particles can collide inside a nonextremal black hole in such a way that the energy $E_{c.m.}$ in their centre of mass frame becomes as large as one likes. We show that this effect can be understood with the help of a simple analogy with particle collisions in flat space-time. As the two-dimensional part of near-horizon geometry inside a black hole is described by the flat Milne metric, the results have a general character. Full classification of scenarios with unbound $E_{c.m.}$ is suggested. Some scenarios of this kind require proximity of collision to the bifurcation point, but for some other ones this is not necessary.

PACS numbers: 04.70.Bw, 97.60.Lf

Keywords: BSW effect, inner black hole horizon, Milne metric

I. INTRODUCTION

The Bañados-Silk-West effect (the BSW effect) consists in getting arbitrarily large energies $E_{c.m.}$ in the centre of mass frame of particles colliding near black holes [1], i.e. in the strong gravitational field. Nonetheless, it turned out that a kinematic nature of the BSW effect outside the event horizon can be revealed in terms of a very simple model of particles colliding in *flat* space-time (see Sec. VI of [2]). Now, we show the existence of analogy of this kind for collisions inside black holes. (We do not touch upon other numerous aspects of the BSW effect.) Thus for the BSW effect near the inner black hole horizon [3] - [7], there exists its counterpart in the flat space-time. One observer explains the BSW effect by the

*Electronic address: zaslav@ukr.net

proximity to the horizon and a special character of trajectories of colliding particles. But another observer does not see the horizon at all, so his explanation should be qualitatively different. Moreover, the two-dimensional part of near-horizon geometry is described by the Milne metric (see below) which is flat, so our consideration relies not on some particular model but has a general character.

It was shown in [6], [7] that one of colliding particles should follow the trajectory that would pass through the bifurcation point where the future and past horizons meet. As such a point does not show up in realistic black holes, one could think that corresponding scenarios of collision looked somewhat academic. Here, we show that, nonetheless, there exists also such a scenario of the BSW effect in which the actual point of collision may be near the horizon far from the bifurcation point. One can hope that this makes the BSW effect near the inner black hole or cosmological horizon more physical.

One reservation is in order. The whole space-time of an eternal black hole consists of the "black hole" and "white hole" parts. I discuss motion of particles from the inner non-static region to the outer static one that corresponds to the white hole region. However, for brevity and in accordance with tradition, I use the term "black hole" anyway. According to the Novikov's classification [8], this is the so-called T_+ region. The pictures describing collision are presented on Fig. 1 and Fig. 2 where the most interesting cases are drawn and the trajectories of the colliding particles, horizons and bifurcation point O are indicated (see for details below).

II. MINKOWSKI AND MILNE METRICS

Let us consider the metric of a spherically symmetric black hole

$$ds^2 = -f dt^2 + \frac{dr^2}{f} + r^2(d\theta^2 + \sin^2\theta d\phi^2). \quad (1)$$

Here, it is assumed that $g_{00}g_{11} = -1$ that does not affect the essence of matter but simplifies formulas. It is implied that there is a horizon at $r = r_h$, so $f(r_h) = 0$. We are interested in the region inside the horizon, so $r \leq r_h$. Near the horizon, we can exploit the Taylor expansion

$$f = f_1(r - r_h) + O((r - r_h)^2), \quad (2)$$

where $f_1 > 0$. Then, omitting the angular part of the metric irrelevant in the present

context, we have near the horizon

$$ds^2 \approx f_1(r_h - r)dt^2 - \frac{dr^2}{f_1(r_h - r)}. \quad (3)$$

In our region, the coordinate r has a time-like character, t is a space-like. Making the substitution

$$r_h - r = \frac{f_1}{4}\tilde{t}^2, \quad t_h - t = \frac{2\tilde{x}}{f_1}, \quad (4)$$

we arrive at the metric

$$ds^2 = -d\tilde{t}^2 + \tilde{t}^2 d\tilde{x}^2. \quad (5)$$

In other words, a nonextremal black hole metric inside the horizon can be approximated in the near-horizon region by the so-called Milne metric (5). This is a counterpart to the well-known fact that outside the horizon the metric of a nonextremal black hole can be approximated (in the two-dimensional subspace) by the Rindler metric.

The metric (5) is flat. It can be obtained from the Minkowski one

$$ds^2 = -dt^2 + dx^2, \quad (6)$$

with the help of the coordinate transformations

$$x = \tilde{t} \sinh \tilde{x}, \quad (7)$$

$$t = \tilde{t} \cosh \tilde{x}. \quad (8)$$

We are interested in the lower quadrant of the entire plane, where

$$t < 0, |x| < |t|. \quad (9)$$

The inverse transformation reads

$$\tilde{t}^2 = t^2 - x^2, \quad (10)$$

$$\tanh \tilde{x} = \frac{x}{t}. \quad (11)$$

There are two horizons in the metric (5): the right horizon $x = -t$, where

$$\tilde{t} = 0, \tilde{x} = -\infty, \quad (12)$$

and the left one $x = +t$, where

$$\tilde{t} = 0, \tilde{x} = +\infty. \quad (13)$$

There is also the "bifurcation point", where both horizons meet, so $x = 0 = t$,

$$\tilde{t} = 0, \quad |\tilde{x}| < \infty. \quad (14)$$

This is point O on figs.1 and 2.

The metric (5) has a space-like Killing vector which can be written in these coordinates as

$$\xi^\mu = (0, 1). \quad (15)$$

The corresponding momentum $X = mu_\mu \xi^\mu$ (m is the particle's mass) is conserved. Here, $u^\mu = \frac{dx^\mu}{d\tau}$ is the four-velocity, τ is the proper time. It follows from the geodesic equations (in which $m = 1$) that

$$\frac{d\tilde{x}}{d\tau} = \frac{X}{\tilde{t}^2}, \quad (16)$$

$$\frac{d\tilde{t}}{d\tau} = -\frac{Z}{\tilde{t}} > 0, \quad Z = \sqrt{X^2 + \tilde{t}^2}, \quad (17)$$

so that

$$\frac{d\tilde{x}}{d\tilde{t}} = -\frac{X}{Z\tilde{t}}. \quad (18)$$

After integration, one finds that

$$\tilde{t} = \frac{X}{\cosh \tilde{x}_0 (V \cosh \tilde{x} - \sinh \tilde{x})} = \frac{x_0}{\sinh \tilde{x} - V \cosh \tilde{x}}, \quad (19)$$

$$V = \tanh \tilde{x}_0, \quad (20)$$

$$X = -x_0 \cosh \tilde{x}_0, \quad (21)$$

where \tilde{x}_0 and x_0 are constants. It follows from (21) that

$$X = -x_0 E, \quad E = \frac{1}{\sqrt{1 - V^2}}. \quad (22)$$

With the help of (7), (8), one can recognize in (19) the standard equation of motion in the Minkowskian coordinates

$$x - Vt = x_0. \quad (23)$$

Here, V has the meaning of velocity, E being the energy.

The frame (5) corresponds to the observer (mentioned in Introduction) who sees the horizon while frame (6) corresponds to the observer who does not. In what follows, we discuss properties of collisions in both Milne and Minlowski frames related by coordinate transformations (7), (8) and (10), (11). It is supposed that colliding particles follow geodesics which are described by eq. (19) in the Milne frame and eq. (23) in the Minkowski frame.

III. COLLISION OF TWO PARTICLES: GENERAL FORMULAS

Let particles 1 and 2 with the momenta X_1 and X_2 , four-velocities u_1^μ and u_2^μ , masses m_1 and m_2 collide. Then, the energy in the centre of mass frame

$$E_{c.m.}^2 \equiv -(m_1 u_1^\mu + m_2 u_2^\mu)(m_1 u_{1\mu} + m_2 u_{2\mu}) = m_1^2 + m_2^2 + 2m_1 m_2 \gamma, \quad (24)$$

where the Lorentz factor of relative motion is

$$\gamma = -u_{1\mu} u_2^\mu. \quad (25)$$

Calculating γ in the frame (5), one can obtain from (16), (17), (25) that

$$\gamma = \frac{Z_1 Z_2 - X_1 X_2}{\tilde{t}^2}, \quad (26)$$

where $Z_{1,2}$ are given by eq. (17), $m_1 = m_2 = 1$ for simplicity. In the Minkowski frame, where

$$u^\mu = \frac{1}{\sqrt{1-V^2}}(1, V), \quad (27)$$

(25) can be rewritten as

$$\gamma = E_1 E_2 (1 - V_1 V_2). \quad (28)$$

In the point of collision,

$$\tilde{t}_1 = \tilde{t}_2 = \tilde{t}_c, \quad \tilde{x}_1 = \tilde{x}_2 = \tilde{x}_c, \quad (29)$$

we obtain from (19) that

$$\tanh \tilde{x}_c = \frac{[(x_0)_2 V_1 - (x_0)_1 V_2]}{[(x_0)_2 - (x_0)_1]}. \quad (30)$$

IV. STRUCTURE OF THE LIGHT CONE AND THE BSW EFFECT

Calculation of the Lorentz factor γ can be also described in the geometric terms on the basis of the approach of [7] and [9]. Let us introduce in a given point two independent light-like basis vectors l^μ and N^μ . It is convenient to normalize them according to $l^\mu N_\mu = -1$. The four-velocity u_i^μ of each particle ($i = 1, 2$) can be expanded as

$$u_i^\mu = \beta_i N^\mu + \frac{l^\mu}{2\alpha_i}. \quad (31)$$

Then, the quantity (25) can be written as

$$\gamma = \frac{1}{2} \left(\frac{\beta_1}{\alpha_2} + \frac{\beta_2}{\alpha_1} \right). \quad (32)$$

Here,

$$\beta = -l_\mu u^\mu, \alpha = -\frac{1}{2}(N_\mu u^\mu)^{-1}. \quad (33)$$

The choice of vectors l^μ and N^μ is ambiguous, one can change them according to $l^\mu \rightarrow \lambda l^\mu$, $N^\mu \rightarrow \lambda^{-1} N^\mu$. However, this entails the transformation $\beta_i \rightarrow \lambda \beta_i$, $\alpha_i \rightarrow \lambda \alpha_i$, so that (32) remains intact. Let us choose the vectors according to

$$\tilde{l}^\mu = (-\tilde{t}, 1), \quad (34)$$

$$\tilde{N}^\mu = \frac{1}{2} \left(-\frac{1}{\tilde{t}}, -\frac{1}{\tilde{t}^2} \right). \quad (35)$$

It is convenient to introduce light-like coordinates

$$\eta = t + x, \zeta = t - x. \quad (36)$$

Then, the same vectors in the Minkowski frame are equal to

$$l^\mu = \zeta(-1, 1), \quad (37)$$

$$N^\mu = \frac{1}{2\zeta}(-1, -1), \quad (38)$$

where we used (10) in the calculation of N^μ .

Calculating the coefficients with the help of eqs. (16), (17), we obtain that $\beta = \alpha$, where

$$\beta = Z - X. \quad (39)$$

In the Minkowski frame, using (27) one finds a simple expression for β in terms of velocity:

$$\beta = -\frac{\zeta(1+V)}{\sqrt{1-V^2}} = \zeta \sqrt{\frac{1-|V|}{1+|V|}}. \quad (40)$$

V. NEAR-HORIZON COLLISIONS

With these general formulas at hand, we are already able to analyze the conditions that lead to the BSW effect. In what follows, we call a particle critical if $X = 0$ and usual if $X \neq 0$. If X does not vanish precisely but is small, we call a particle near-critical. We are

interested in the cases when γ in (24) can become unbound despite finite $X_{1,2}$. It is seen from (26) that the only possibility of getting unbound γ is to arrange collision with small \tilde{t} . Then, either collision occurs near the bifurcation point (14) or near the horizon (say, the right one) (12). We discuss different cases depending on X_i and will show which of them correspond to the bifurcation point or the horizon.

A. $X_1 X_2 < 0$

For small \tilde{t}_c , it follows from (17), (26) that

$$\gamma \approx \frac{2|X_1 X_2|}{\tilde{t}_c^2}. \quad (41)$$

As we try to arrange the conditions for the BSW effect, we assume that X_1 and X_2 are separated from zero, so both particles are usual. It would seem that the BSW effect occurs according to (41). However, more careful inspection shows that this is not necessary so (see below). Small \tilde{t}_c imply either the vicinity of the right or left horizon (then, $|\tilde{x}_c| \rightarrow \infty$ according to (12), (13)) or the vicinity of the bifurcation point (14) (\tilde{x}_c is finite). We will consider these cases separately.

1. Collision near the horizon

Let us try to arrange collision near, say, the right horizon. It follows from (12) and (30) that

$$V_1 = -1 + (1 + V_2) \frac{(x_0)_1}{(x_0)_2}. \quad (42)$$

As, by assumption, X_1 and X_2 have different signs, $(x_0)_1$ and $(x_0)_2$ also have different signs according to (22). Then, it follows from eq. (42) that $V_1 < -1$ that is impossible. (In a similar way, near the left horizon we would obtain $V_1 > 1$.) Thus the condition of collision (30) is inconsistent with $|V_1| < 1$. Therefore, collision on the horizon cannot occur. In the intermediate point with $\tilde{t}_c \neq 0$ it is possible, but γ is finite there, so there is no the BSW effect. This is in agreement with previous studies [3] - [7].

2. *Scenario A: collision near the bifurcation point*

Near the bifurcation point, t and x are small, so according to (23), $(x_0)_1$ and $(x_0)_2$ are also small. As by assumption, X_1 and X_2 are separated from zero, (22) entails that $E_{1,2} \rightarrow \infty$, so $|V_{1,2}| \rightarrow 1$. As is explained above, $(x_0)_1$ and $(x_0)_2$ have different signs. Then, by substitution into (30), we see that if $V_1 \approx 1 \approx V_2$ or $V_1 \approx -1 \approx V_2$, it turns out that $|\tilde{x}_c| \rightarrow \infty$ contrary to the property (14). However, it is possible to have $V_1 \approx -V_2 \approx \pm 1$. As in the quadrant under discussion inequality (9) holds, it is clear from (23) that for $V_i \approx +1$, we have $(x_0)_i > 0$, so $X_i < 0$ from (22) ($i = 1, 2$). In a similar way, for $V_i \approx -1$, we have $(x_0)_i < 0$ and $X_i > 0$. Considering both subcases, we obtain in the point of collision:

a) $V_1 \approx +1$, $V_2 \approx -1$, $X_1 < 0$, $X_2 > 0$.

Then, in the limit $\tilde{t}_c \rightarrow 0$, one obtains from (40) that

$$\beta_1 \approx 2|X_1|, \beta_2 \approx \frac{\tilde{t}_c^2}{2X_2}. \quad (43)$$

From (32) and (43), eq. (41) is recovered. From the other hand, (28) gives us

$$\gamma \approx 2E_1E_2. \quad (44)$$

Now, $(x_0)_1(x_0)_2 \approx x^2 - t^2 = -\tilde{t}^2$, where we used (10). Therefore, (41) agrees with (44). Here, both E_1 and E_2 grow unbound. However, X_1 and X_2 are finite!

b) $V_1 \approx -1$, $V_2 \approx +1$, $X_1 > 0$, $X_2 < 0$,

$$\beta_2 \approx 2|X_2|, \beta_1 \approx \frac{\tilde{t}_c^2}{2X_1}, \quad (45)$$

eq. (44) holds.

B. $X_1X_2 \geq 0$

First, let both X_1 and X_2 be separated from zero (both particles are usual). We are interesting in the case of small \tilde{t} only. Then, it is seen from (17) that $Z_{1,2} \approx |X_{1,2}| + \frac{\tilde{t}^2}{2|X_{1,2}|}$. As a consequence, the gamma factor in (26) is finite, so there is no the BSW effect.

For γ to be unbound, it is necessary that (i) collision occur for small \tilde{t}_c , (ii) one particle (say, particle 1) be critical or near-critical and particle 2 be finite. For definiteness, we take particle 1 to be precisely critical, so

$$X_1 = 0. \quad (46)$$

It is seen from (21) that in this case

$$(x_0)_1 = 0. \quad (47)$$

Then, one can obtain from (10), (23), (30)

$$x_c = V_1 t_c \quad (48)$$

$$V_1 = \tanh \tilde{x}_c, \quad (49)$$

$$\tilde{t}_c = t_c \sqrt{1 - V_1^2}, \quad (50)$$

$$X_2 = |t_c| (V_1 - V_2) E_2 = \frac{|\tilde{t}| (V_1 - V_2) E_2}{\sqrt{1 - V_1^2}}. \quad (51)$$

Here, according to (36), (23) and (47), $\zeta_c = t_c(1 - V_1)$. Then, it follows from (39), (40) and (51) that

$$\beta_1 = |\tilde{t}_c| = \frac{X_2 \sqrt{1 - V_1^2}}{(V_1 - V_2) E_2}. \quad (52)$$

$$\beta_2 = |\tilde{t}_c| \sqrt{\frac{1 - V_1}{1 + V_1}} (1 + V_2) E_2 = \frac{X_2 (1 - V_1) (1 + V_2)}{V_1 - V_2} \quad (53)$$

Eq. (26) simplifies to

$$\gamma = \frac{Z_2}{|\tilde{t}_c|}. \quad (54)$$

Below, we list the results of analysis and enumerate different cases that give rise to unbound γ . We indicate the relevant quantities in terms of both frames (6) and (5). In all cases, $\tilde{t} \rightarrow -0$, $X_2 \neq 0$, β_1 is given by eq. (52), eq. (54) gives us

$$\gamma \approx \frac{X_2}{|\tilde{t}_c|}. \quad (55)$$

1. Scenario B: collision near the bifurcation point

According to (14), near the bifurcation point \tilde{x}_c is finite. Therefore, it follows from (49) that $|V_1| < 1$. For a usual particle, eq. (51) holds. It is seen from it that, to reconcile finite nonzero X_2 with small x_c , we must have large E_2 . Then, it follows from (22) that $|V_2| \rightarrow 1$. There are two subcases depending on the sign of V_2 .

a) $V_2 \approx -1$. Then, it follows from (51) that $X_2 > 0$. It is seen from (17), (39) and (53) that

$$\beta_2 \approx \frac{\tilde{t}_c^2}{2X_2} \approx \frac{X_2 (1 - V_1) (1 + V_2)}{1 + V_1}, \quad (56)$$

so in (32), (28)

$$\gamma \approx \frac{\sqrt{1+V_1}}{\sqrt{2}\sqrt{1-V_1}\sqrt{1+V_2}} \rightarrow \infty. \quad (57)$$

b) $V_2 \approx +1$. Then, it follows from (51) that $X_2 < 0$. Eqs. (39) - (53) give us

$$\beta_1 \approx \frac{|X_2|}{E_2} \sqrt{\frac{1+V_1}{1-V_1}} \quad (58)$$

$$\beta_2 \approx 2|X_2|. \quad (59)$$

whence

$$\gamma \approx \frac{\sqrt{1-V_1}}{\sqrt{2}\sqrt{1+V_1}\sqrt{1-V_2}} \rightarrow \infty. \quad (60)$$

2. Scenario C: collision near the horizon

Near the horizon, $|\tilde{x}_c| = \infty$ according to (12), (13). Then, it follows from (49) that $|V_1| \rightarrow 1$. The value of t_c is, generally speaking, separated from zero, \tilde{t}_c in (50) is small due to the second factor. Therefore, collision can occur far from the bifurcation point. It follows from (51) with finite X_2 that E_2 is finite, so $|V_2| < 1$. Now, there are two subcases depending on the sign of V_1 .

a) $V_1 \approx -1$, $\tilde{x}_c \rightarrow -\infty$. Then, it follows from (51) that $X_2 < 0$. According to (48), collision occurs near the right horizon $x = -t$. We see from (52) that

$$\beta_1 \approx \frac{\sqrt{2}|X_2|\sqrt{1+V_1}\sqrt{1-V_2}}{\sqrt{1+V_2}}, \quad (61)$$

for β_2 eq. (59) holds.

Then, (32) gives us

$$\gamma \approx \frac{\sqrt{1+V_2}}{\sqrt{2}\sqrt{1+V_1}\sqrt{1-V_2}} \rightarrow \infty. \quad (62)$$

b) $V_1 \approx +1$, $\tilde{x}_c \rightarrow +\infty$, now $X_2 > 0$ and

$$\beta_1 \approx \frac{\sqrt{2}X_2\sqrt{1-V_1}\sqrt{1+V_2}}{\sqrt{1-V_2}} \quad (63)$$

$$\beta_2 \approx \frac{\tilde{t}_c^2}{2X_2} \approx \frac{(1+V_2)(1-V_1)X_2}{(1-V_2)}. \quad (64)$$

$$\gamma \approx \frac{\sqrt{1-V_1}}{\sqrt{2}\sqrt{1+V_2}\sqrt{1-V_1}} \rightarrow \infty. \quad (65)$$

For completeness, we discuss briefly the remaining cases. If $X_1 = 0 = X_2$ (two critical particles), it is seen from (26) that $\gamma = 1$, so this degenerate case is uninteresting. Also, there is no BSW effect if $X_i = O(\tilde{t}_c)$ (both particles are near-critical).

C. Collision of near-critical and usual particles

In scenarios B and C, we considered the case when one particle is precisely critical. If particle 1 is near-critical and particle 2 is usual, it follows from (26) that in the limit $\tilde{t}_c \rightarrow 0$,

$$\gamma = \frac{1}{2} \left(\left| \frac{X_1}{X_2} \right| + \left| \frac{X_2}{X_1} \right| \right). \quad (66)$$

Taking also into account the above results for scenarios with collisions near the horizon, one can write

$$\lim_{X_1 \rightarrow 0} \lim_{\tilde{t}_c \rightarrow 0} \gamma = \lim_{\tilde{t}_c \rightarrow 0} \lim_{X_1 \rightarrow 0} \gamma = \infty. \quad (67)$$

In other words, in scenarios B and C the BSW effect can be realized in two basic ways: either (i) particle 1 is critical, collision happens near the horizon (see Fig. 1) or (ii) collision happens on the horizon itself, particle 1 is near-critical (see Fig. 2).

For collision on the horizon (say, the right one), it is seen from (23) with $x = t$ that $(x_0)_i = t(1 - V_i)$. As $V_i < 1$ and $t < 0$, we have $(x_0)_i < 0$ and, according to (21), $X_i > 0$. In a similar way, $X_i < 0$ for both particles if collisions occur on the left horizon. Thus $X_1 X_2 > 0$ for collision near the horizon. There is no such a restriction for collisions near the bifurcation point.

VI. SUMMARY OF RELEVANT SCENARIOS

In Table 1 below, we summarize the results of analysis.

Table 1. Types of collisions leading to the BSW effect for the Milne model.

Scenario	V_1	V_2	X_1	X_2	β_1	β_2	Location
Aa	$\approx +1$	≈ -1	< 0	> 0	$2 X_1 $	$\sim \tilde{t}_c^2 \ll \beta_1$	Bifurcation point
Ab	≈ -1	$\approx +1$	> 0	< 0	$\sim \tilde{t}_c^2$	$2 X_2 \gg \beta_1$	Bifurcation point
Ba	intermediate	≈ -1	0	> 0	$\sim \tilde{t}_c $	$\sim \tilde{t}_c^2 \ll \beta_1$	Bifurcation point
Bb	intermediate	$\approx +1$	0	< 0	$\sim \tilde{t}_c $	$2 X_2 \gg \beta_1$	Bifurcation point
Ca	≈ -1	intermediate	0	< 0	$\sim \tilde{t}_c $	$2 X_2 \gg \beta_1$	Horizon
Cb	$\approx +1$	intermediate	0	> 0	$\sim \tilde{t}_c $	$\sim \tilde{t}_c^2 \ll \beta_1$	Horizon

We indicate only scenarios that obey two criteria: (i) γ is unbound, (ii) two particle indeed meet in the same point, so eq. (29) is satisfied. To simplify presentation, we assumed that particle 1 in scenarios B and C is exactly critical. This table gives us the full list of

cases when the Lorentz factor of relative motion γ grows unbound for finite X_i . Strictly speaking, there is one more case not shown in the table since it is trivial. It corresponds to infinitely large momenta X_i . In scenario A, both particles are usual. In all other scenarios particle 1 is critical (or near-critical), particle 2 is usual.

In all cases, according to (32), $\gamma \approx \frac{1}{2} \frac{\beta_2}{\beta_1}$, if $\beta_2 \gg \beta_1$ and $\gamma \approx \frac{1}{2} \frac{\beta_1}{\beta_2}$, if $\beta_1 \gg \beta_2$.

The fact that in scenario Bb the coefficient $\beta_1 \rightarrow 0$ for the critical particle and $\beta_2 \neq 0$ for a usual one is in agreement with general properties of the bifurcation point relevant in the context of the BSW effect [7]. Meanwhile, table 1 contains also some new possibilities. In scenario Ba, both β_1 and β_2 vanish as the bifurcation point is approached. However, this occurs with essential different rates, so γ becomes unbound according to (32). In scenario C, t_c and $x_c \approx -t_c$ do not vanish, so collision happens far from the bifurcation point.

If, instead of collisions in flat space-time (which turned out to be useful methodical tool), we consider true black holes posing the electric charge or angular momentum, X_i are not conserved [6]. Classification itself retains its validity, provided X_i are taken in the vicinity of the horizon. In a general form, omitting details, the corresponding table has the following structure.

Table 2. General types of collisions leading to the BSW effect inside black holes.

Scenario	particle 1	particle 2	$X_1 X_2$	Location
A	usual	usual	< 0	Bifurcation point
B	critical or near-critical	usual	0 or small	Bifurcation point
C	critical or near-critical	usual	0 or > 0 small	Horizon

A. Comparison with previous studies

It is instructive to compare the present results with those in our previous studies [6], [7]. Scenario A was considered in [6] where it was displayed on Fig. 7. Scenario Bb was discussed in [7], so case Ba extends the list of possibilities. Scenario C was actually mentioned earlier in Sec. V B 2 of [6] (displayed on Fig. 7 there) but identified not quite accurately in that, actually, one particle should be near-critical, not simply usual.

Now, having sorted out all possible cases systematically, we obtained the comprehensive list of relevant scenarios.

VII. DISCUSSION AND CONCLUSION

We have managed to construct classification of all possible scenarios of collisions of particles near the inner horizon leading to the indefinite growth of $E_{c.m.}$. This is done with the help of an elementary model of two particles collision in flat space-time. In the Milne frame, the BSW effect happens due to the existence of the horizon and a special character of trajectories. In the Minkowski frame, there is no horizon. There, the effect is due to the fact that a rapid particle hits a slow or motionless one (or there is head-on collision of two rapid particles like in Scenario A).

In true black hole metrics the whole situation is more complicated. However, locally, in the small vicinity of the horizon from inside, the Milne metric can be considered as a good approximation to the black hole metric. Therefore, our consideration is quite generic and is applicable to the BSW effect inside true black holes. In this context, "trivializing" the effect by appealing to the Minkowski space-time, tangent to a given point, is a tool to understand the BSW effect inside black holes where both the effect itself and its properties were not so obvious (see discussion in [3] - [7]). In other words, it is the simplified Milne metric that enabled us to construct Table 2 of possible scenarios in a general case.

Scenario C of collisions tells us that the high energy collision can occur far from the bifurcation point, its very existence is not mandatory at all. This makes this version of the BSW effect more physical: it can manifest itself any time a particle with the fine-tuned parameters crosses the horizon in the direction from the inner nonstatic region to the outer static one, be it the inner black hole horizon, the cosmological or the isolated one [10].

-
- [1] M. Bañados, J. Silk and S.M. West, Phys. Rev. Lett. **103**, 111102 (2009) [arXiv:0909.0169].
 - [2] O. B. Zaslavskii, Phys. Rev. D **88**, 104016 (2013) [arXiv:1301.2801].
 - [3] A. A. Grib and Yu.V. Pavlov, Astropart. Phys. **34**, 581 (2011) [arXiv:1001.0756].
 - [4] A. A. Grib and Yu.V. Pavlov, Gravitation and Cosmology **17**, 42 (2011) [arXiv:1010.2052].
 - [5] K. Lake, Phys. Rev. Lett. **104**, 259903(E) (2010).
 - [6] O. B. Zaslavskii, Phys. Rev. D **85**, 024029 (2012) [arXiv:1110.5838].
 - [7] O. B. Zaslavskii, Int. Journ. Mod. Phys. D. **22**, 1350044 (2013) [arXiv:1203.5291].
 - [8] I. D. Novikov, Commun. Sternberg Astron. Inst. Moscow **132**, 3 (1964); **132**, 43 (1964)

(republished in Gen. Relativ. and Gravit. **33**, 2259 (2001)).

- [9] O. B. Zaslavskii, Class. Quantum Grav. **28**, 105010(2011) [arXiv:1011.0167].
- [10] A. Ashtekar and B. Krishnan, Liv. Rev. Rel. **7** 10 (2004) [arXiv:gr-qc/0407042].

Figures

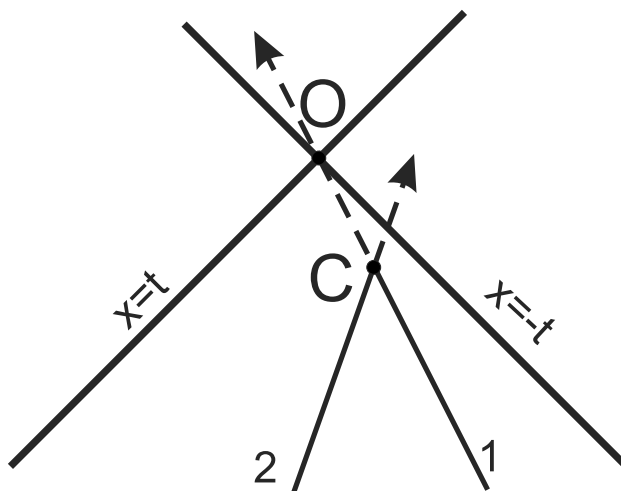


FIG. 1: Collision between the critical particle 1 and a usual particle 2 near the horizon.

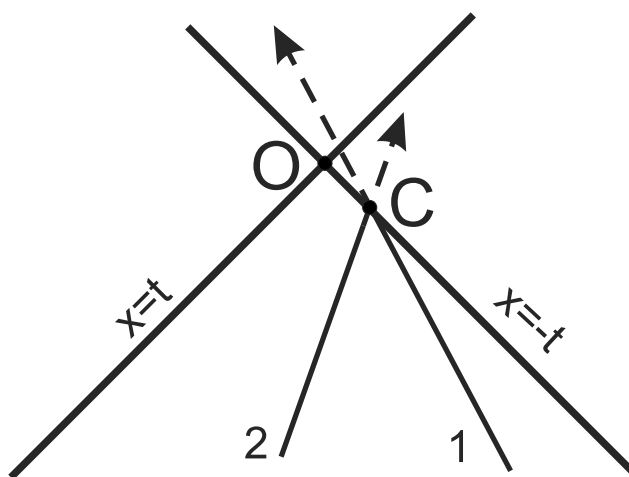


FIG. 2: Collision between the near-critical particle 1 and a usual particle 2 on the horizon.